Desiccation-Induced Structuralization and Glass Formation of Group 3 Late Embryogenesis Abundant Protein Model Peptides

ARTICLE *in* BIOCHEMISTRY · DECEMBER 2009

Impact Factor: 3.02 · DOI: 10.1021/bi901745f · Source: PubMed

8 AUTHORS, INCLUDING:

Takahiro Kikawada
National Institute of Agrobiological Sciences
68 PUBLICATIONS **924** CITATIONS
SEE PROFILE

Tsuyoshi Takahashi
Gunma University
42 PUBLICATIONS **422** CITATIONS
SEE PROFILE

Hisakazu Mihara
Tokyo Institute of Technology
233 PUBLICATIONS **3,471** CITATIONS
SEE PROFILE

BIOCHEMISTRY
including biophysical chemistry & molecular biology
Article

Biochemistry **2010,** *49,* 1093–1104 1093
DOI: 10.1021/bi901745f

Desiccation-Induced Structuralization and Glass Formation of Group 3 Late Embryogenesis Abundant Protein Model Peptides†

Tempei Shimizu,‡ Yasushi Kanamori,§ Takao Furuki,‡ Takahiro Kikawada,§ Takashi Okuda,∥ Tsuyoshi Takahashi,∥ Hisakazu Mihara,§ and Minoru Sakurai*,‡

‡*Center for Biological Resources and Informatics, Tokyo Institute of Technology, 4259-B-62, Nagatsuta-cho, Midori-ku, Yokohama 226-8501, Japan,* §*National Institute of Agrobiological Sciences* (*NIAS*)*, 1-2, Ohwashi, Tsukuba 305-8634, Japan, and* ∥*Department of Bioengineering, Graduate School of Bioscience and Biotechnology, Tokyo Institute of Technology, 4259-B-40, Nagatsuta-cho, Midori-ku, Yokohama 226-8501, Japan*

Received October 10, 2009; Revised Manuscript Received December 14, 2009

ABSTRACT: Anhydrobiotic (i.e., life without water) organisms are known to produce group 3 late embryogenesis abundant (G3LEA) proteins during adaptation to severely water-deficient conditions. Their primary amino acid sequences are composed largely of loosely conserved 11-mer repeat units. However, little information has been obtained for the structural and functional roles of these repeat units. In this study, we first explore the consensus sequences of the 11-mer repeat units for several native G3LEA proteins originating from anhydrobiotic organisms among insects (*Polypedilum vanderplanki*), nematodes, and plants. Next, we synthesize four kinds of model peptides (LEA models), each of which consists of four or two repeats of the 11-mer consensus sequences for each of the three organisms. The structural and thermodynamic properties of the LEA models were examined in solution, in dehydrated and rehydrated states, and furthermore in the presence of trehalose, since a great quantity of this sugar is known to be produced in the dried cells of most anhydrobiotic organisms. The results of Fourier transform infrared (FTIR) spectroscopic measurements indicate that all of the LEA models transform from random coils to α-helical coiled coils on dehydration and return to random coils again on rehydration, both with and without trehalose. In contrast, such structural changes were never observed for a control peptide with a randomized amino acid sequence. Furthermore, our differential scanning calorimetry (DSC) measurements provide the first evidence that the above 11-mer motif-containing peptides themselves vitrify with a high glass transition temperature (> 100 °C) and a low enthalpy relaxation rate. In addition, they play a role in reinforcing the glassy matrix of the coexisting trehalose. On the basis of these results, we discuss the underlying mechanism of G3LEA proteins as desiccation stress protectants.

Late embryogenesis abundant (LEA) proteins were initially discovered more than 2 decades ago in orthodox seeds (*1*−*3*), in which they represent more than 4% of cellular proteins (*4*, *5*). Several types of LEA proteins and their genes have since been reported for many plant species, and LEA proteins have been classified into at least four groups based on their amino acid sequence (*6*−*8*). Among them, group 3 LEA (G3LEA)[1] proteins and genes are known to be upregulated in particular tissues of vegetative plants (*7*, *8*). They seem to play important roles in induction and maintenance of a temporary death-defying state named "anhydrobiosis" or "cryptobiosis" (*9*) because they accumulate in response to the stress of water deficit (*10*−*15*).

A major characteristic of G3LEA proteins is the occurrence of several loosely conserved 11-mer amino acid units in the primary sequence (*16*). In an early study, the consensus motif of the repeated 11-mer units of G3LEA proteins was identified as "TAQAAKEKAGE" (*17*). Subsequently, G3LEA proteins were found in a diverse collection of plants. Currently, the consensus motif of the 11-mer units for plant G3LEA proteins is recognized as "ΦΦΩXΦΨΩΨΦXΩ", where Φ, Ω, and Ψ represent hydrophobic residues, negatively charged or amide residues, and positively charged residues, respectively, and X represents a nonspecifically conserved amino acid residue (*17*, *18*).

In recent years, G3LEA protein genes were also found in many nonplant species such as prokaryotes (*14*, *18*), nematode (*19*−*21*), and rotifers (*22*, *23*). In an anhydrobiotic nematode, *Aphelenchus avenae*, a G3LEA protein gene named *Aav-lea-1* has features similar to those of typical plant G3LEA protein genes (*19*). However, the consensus 11-mer motif in the corresponding protein, AavLEA1, "KAAEF(T)KQRAGE", is slightly different from the pattern "ΦΦΩXΦΨΩΨΦXΩ" found for plant LEA proteins (*24*). More recently, three G3LEA protein genes, *PvLea1, PvLea2*, and *PvLea3*, were cloned from larvae of the sleeping chironomid, *Polypedilum vanderplanki* (*25*). All *PvLea* genes were upregulated in response to desiccation and salinity stress, and the corresponding proteins possessed characters typical of G3LEA proteins such as high hydrophilicity and heat solubility. In addition, the majority of their amino acid sequences was also shown to be composed of 11-mer repeat units similar to

†This work was supported in part by the Promotion of Basic Research Activities for Innovative Biosciences (PROBRAIN) and also in part by Grants-in-Aid for Scientific Research (No. 21370068 and No. 21688004) from the Ministry of Education, Culture, Sports, Science, and Technology of Japan.

*Corresponding author. Tel: +81-45-924-5795. Fax: +81-45-924-5795. E-mail: msakurai@bio.titech.ac.jp.

[1]Abbreviations: G3LEA, group 3 late embryogenesis abundant; FTIR, Fourier transform infrared; DSC, differential scanning calorimetry; PvLEA, NeLEA, and PlLEA, 22- or 44-mer peptides constructed from the LEA models originating from insects (*Polypedilum vanderplanki*), nematodes, and plants, respectively; ΔH_{relax}, enthalpy relaxation; T_g, glass transition temperature.

Published on Web 12/22/2009

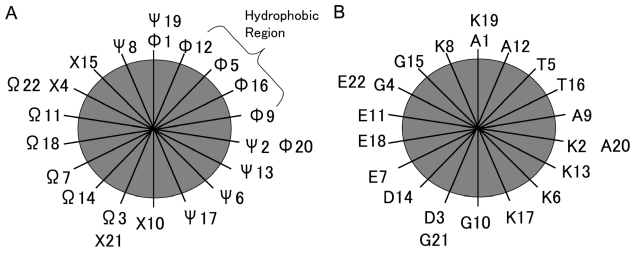

FIGURE 1: α-Helical wheel for the 11-mer repeat units in G3LEA proteins. (A) Result for the consensus sequence obtained for plant G3LEA proteins, where Dure's notations are used for amino acid classification (see text). (B) Results for the consensus sequence obtained for G3LEA proteins of *P. vanderplanki* (this work).

those of the typical plant G3LEA proteins. From an evolutionary viewpoint, it is of great interest to compare the 11-mer repeat sequences of G3LEA proteins from different anhydrobiotic organisms in greater detail. For this purpose, the consensus sequences of the 11-mer repeat units need to be explored for each organism with a common statistical protocol.

If the polypeptide chains composed of the above-mentioned 11-mer units form α-helical structures, they are expected to have an amphiphilic character due to a hydrophobic stripe formed by the apolar residues at the positions 1, 2, 5, and 9 and a wider hydrophilic stripe formed by the polar residues at the positions 3, 6, 7, 8, and 11 (Figure 1A). Early computer modeling studies predicted that such amphiphilic α-helices dimerized in a right-handed coiled-coil arrangement through the interactions of the hydrophobic stripes (*17*). Later, the formation of a coiled-coil-like structure was observed for AavLEA1 and a mitochondrial G3LEA protein from measurements of FTIR spectra (*26*, *27*), in which there appeared at 1600−1700 cm^{-1} several peaks characteristic of coiled coils. In both cases, although the proteins were unstructured in solution, they transformed to coiled coil on drying: such structural changes occurred reversibly. On the other hand, for a D-7 LEA protein from pollen, the vibration peaks characteristic of coiled coil were not observed in the above fingerprint region, although the structuralization to α-helix and/or β-sheet occurred on drying (*28*). These observations are highly unusual because protein dehydration is most often associated with a loss of structure, together with aggregation, rather than with an increase of structure. It is likely that this intriguing behavior of G3LEA proteins is dependent on the properties of their 11-mer motifs, and it will therefore be of interest to perform experimental or computer simulation studies on these sequences in isolation.

Anhydrobiotic organisms commonly accumulate a high concentration of trehalose or sucrose under desiccation stress (*29*). For example, when an African chironomid, *P. vanderplanki*, is dehydrated slowly, it converts as much as 20% of its dry weight into this molecule (*30*). Thus, *in vivo* G3LEA proteins coexist with these disaccharides, which might affect the structure of the G3LEA protein. Conversely, the proteins are likely to modify the properties (e.g., as glasses) of such coexisting sugars. In fact, an *in vitro* study of a pollen LEA protein indicated that the glassy matrix of sucrose becomes more stable by adding this protein (*28*). In order to understand the function of G3LEA proteins in greater depth, intensive studies on the interaction with sugars are crucial, especially regarding the role of the 11-mer repeat regions.

In this study, we address the following issues: (1) exploration and comparison of the consensus 11-mer motifs of different anhydrobiotic organisms such as plants, nematodes, and an insect, (2) the coiled-coil formation ability of polypeptides containing these consensus 11-mer motifs in the absence and presence of trehalose, and (3) the vitrification properties of these polypeptides themselves and their effect on the glassy matrix of trehalose. Especially for the purpose of issue 2, we here synthesize several model peptides, each of which is composed of four or two 11-mer consensus motifs deduced from the results of issue 1. Their structural and thermodynamic properties were investigated in solution and in dehydrated and rehydrated states by Fourier transform infrared (FTIR) spectroscopy and differential scanning calorimetry. Our recent study pointed out the possibility that the glassy matrix in the dried larvae of *P. vanderplanki* may be made not only from trehalose but also from other component(s) such as G3LEA proteins (*31*). In issue 3, we therefore paid special attention to the glassy property of the binary mixture of trehalose and polypeptides composed of the 11-mer repeat units for this insect. On the basis of the outcome of these investigations, we discuss the intrinsic nature and biological roles of the 11-mer repeat units characteristic of G3LEA proteins.

MATERIALS AND METHODS

Bioinformatic Analyses. To elucidate the differences and similarities of G3LEA proteins among different taxa, we explored the 11-mer models of several G3LEA proteins derived from three phylogenetically divergent anhydrobiotic organisms that belong to Magnoliophyta (i.e., flowering plants), Nematoda, and Insecta. The amino acid sequences of G3LEA proteins of plants and nematodes were obtained from the protein family database (Pfam) 20.0 (http://www.sanger.ac.uk/Software/Pfam/), where LEA_4 (PF02987) is given as a key word referring to the characteristic domain that contains seven or eight repeats of the 11-mer motif of G3LEA proteins. Here, we selected two G3LEA proteins in each of plants and nematodes: for plants, LEA D-7 (Pfam entry number P13939) from *Gossypium hirsutum* (*32*) and LEA 76 (P13934) from *Brassica napus* (*33*), and for nematodes, AavLEA1 (Q95 V77) from an anhydrobiotic nematode, *A. avenae*, and Ce-LEA (O16527) from *Caenorhabditis elegans*. For an anhydrobiotic insect, *P. vanderplanki*, we obtained the following three G3LEA protein genes from GenBank (http://www.ncbi.nlm.nih.gov/sites/entrez?db=protein): PvLEA1 (Accession No. BAE92616), PvLEA2 (BAE92617), and PvLEA3 (BAE92618).

Next, we searched for LEA_4 domains in each primary sequence of the corresponding proteins using the HMMER program in Pfam 20.0. Each LEA_4 domain obtained was divided into 11 consecutive amino acids. The resultant 11-mer fragments were all aligned using CLUSTAL X, which is a multiple sequence alignment program for DNA or protein (*34*). Detailed inspection of such alignment results allowed us to identify where 11-mer repeat units are located in the given LEA_4 domain. Then we calculated the probability of finding a specific type of amino acid at each of the 11 positions and picked up the most frequently occurring amino acid along the sequence. The amino acids were sorted into three groups: (i) hydrophobic residues (Φ: A, I, L, M, and T), (ii) negatively charged or amide residues (Ω: E, D, N, and Q), and (iii) positively charged residues (Ψ: K and R) (*18*). Finally, the percentages of the composition of amino acids for each location in the 11-mer sequence were determined. By analyzing these data, we determined the 11-mer models of the G3LEA protein genes for each organism.

Peptide Synthesis. In order to examine the structural properties of the above 11-mer models, several model peptides (LEA models) consisting of four or two repeats of one of those motifs were synthesized. Hereafter, we denote them as PvLEA-44, PvLEA-22, NeLEA-22, and PlLEA-22, where PvLEA, NeLEA, and PlLEA means the peptides constructed from the LEA models originating from insects (*P. vanderplanki*), nematodes, and plants, respectively, and 44 and 22 represent the number of amino acid residues involved. In addition, we synthesized a control peptide whose amino acid composition is identical with that of the PvLEA-22 but whose sequence is randomized.

All peptides were synthesized according to the solid-phase method based on Fmoc chemistry (*35*). Side chains of Fmoc amino acids were protected by *tert*-butyl (tBu) for "T", "E", and "D" and by *tert*-butyloxycarbonyl (Boc) for "K". Here we used Rink amide MBHA resins for 22-mer and Fmoc-NH-SAL-PEG resins for 44-mer peptides with 2-(1*H*-benzotriazol-1-yl)-1,1,3,3-tetramethyluronium hexafluorophosphate (HBTU, 3 equiv), 1-hydroxybenzotriazole (HOBT, 3 equiv), and diisopropylethylamine (DIEA, 6 equiv) as coupling reagents (*35*).(*5*) The Fmoc group was removed by treatment with *N*-methylpyrrolidone/piperidine (80/20 v/v). After elongation of the amino acids, the resin and the side chain protecting groups were removed by 1 h treatment with trifluoroacetic acid (TFA)/*m*-cresol/thioanisole (40/1/3 v/v). All of the products were precipitated from diethyl ether and collected by centrifugation. Furthermore, they were purified on reverse-phase HPLC (Hitachi L7000, Tokyo, Japan) and subsequently lyophilized in D_2O for FTIR and H_2O for DSC measurements. To identify the final products, their molecular weights were measured by MALDI-TOFMS (Shimadzu KOMPACT MALDI III, Kyoto, Japan).

Disaccharides. Trehalose dihydrate (99.9% purity) was kindly provided by Hayashibara Biochemical Laboratories, Inc. (Okayama, Japan). Before use, it was lyophilized in D_2O and recrystallized from D_2O in a desiccator (relative humidity (RH) 5%) at 25 °C.

Sample Preparation for Physicochemical Measurements. For FTIR measurements, all of the peptides were dissolved in D_2O at ambient temperature for H−D exchange, a treatment necessary for eliminating the H−O−H scissoring vibration peak overlapping the amide I band of the peptide bond. The peptide was dissolved so that the final molar ratio of peptide:D_2O was 1:10000 (5.5 mM). Such a moderate concentration allowed us to accurately monitor the structural changes of the peptides. To examine the interaction between the peptides and trehalose, the sugar was added to this solution; the trehalose/peptide molar ratios ranged from 0 to 5. The dried sample was obtained by placing a droplet (5 μL) of the above peptide solution on a Teflon plate in a desiccator (RH 5%) for 24 h at 25 °C. The residual water content was measured for each dried sample by Karl Fischer titration assay, being found to be approximately 2.0 wt %. The FTIR measurements were started immediately after completion of the sample preparation to avoid the absorption of H_2O into the samples.

For thermodynamic analysis by DSC, we prepared the dried samples for PvLEA-44, PvLEA-22, and the control in the same manner, although without deuterium exchange.

Pure amorphous trehalose used for FTIR measurements was prepared as follows: the trehalose dihydrate crystal was heated to 140 °C, followed by rapid cooling to room temperature.

FTIR Measurements. FTIR spectra were measured using a Fourier transform infrared spectrometer (JASCO FTIR 6100 and IMV-4000, Tokyo, Japan) equipped with a high-sensitivity mercury−cadmium telluride detector. The above aqueous samples were poured between two CaF_2 plates (20 mm (diameter) × 2 mm (thickness)) with a Teflon spacer (50 μm thickness). On the other hand, the dried samples were pressed at approximately 240 kg/cm^2 between two KBr plates (7 × 7 × 1 mm). All of the spectra were obtained in the range 700−4000 cm^{-1} with a spectral resolution of 4 cm^{-1} and 128 scans. In order to investigate the secondary structures of the LEA models, the amide I and amide II absorption bands appearing between 1500 and 1800 cm^{-1}, which arise from the C=O and N−H vibrations of peptide bonds, were analyzed. Their second-derivative spectra were obtained using JASCO (Tokyo, Japan) Spectra Manager Version 2 software.

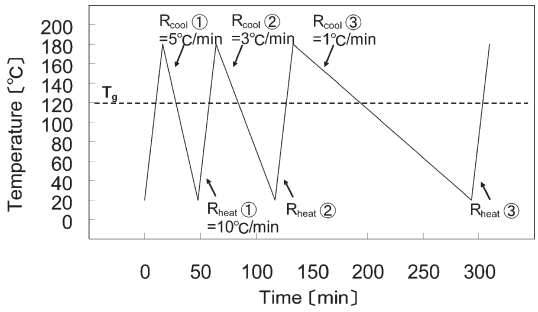

FIGURE 2: Protocol of temperature control in the measurements of enthalpy of relaxation, ΔH_{relax}.

FTIR measurements were also used for observation of the glass transition of several dried samples (PvLEA-22/trehalose mixtures and pure trehalose). Then the sample temperature was heated to 180 °C at a constant rate of 1 °C/min, and we monitored the shift of the maximal peak position, ν_{high} cm^{-1}, in the high frequency region between 3500 and 3300 cm^{-1}, where mainly the O−H and N−H stretching vibration bands appear. The inflection point of the linear regression lines against temperature was determined as the glass transition, T_g (*28*, *36*, *37*).

DSC Measurements. All DSC measurements were carried out using a Pyris Diamond DSC instrument (Perkin-Elmer Japan Co., Tokyo, Japan). The apparatus was calibrated using indium. Dried peptide samples (PvLEA-44, PvLEA-22, control) having a total mass of approximately 5.0 mg were placed in 15 μL silver DSC pans, which were then hermetically sealed. An empty silver pan was used as a reference. Dry nitrogen gas was streamed at 20 mL/min to purge the DSC furnace. All DSC samples were cooled to 20 °C from room temperature, and a first scan to 180 °C at 10 °C/min was performed in order to erase the thermal history. After the first scan, each sample was immediately cooled to 20 °C, and then a second heating scan was started, heating to 180 °C at 10 °C/min. The glass transition was analyzed from the second heating scan.

To evaluate the enthalpy relaxation of the dried peptide sample, DSC measurements were carried out according to the protocol recently proposed by Kawai et al. (*38*). First, the sample temperatures were elevated to 180 at 10 °C/min and immediately afterward cooling runs to 20 °C were performed at a desired cooling rate, R_{cool}. The glass transition and enthalpy relaxation (ΔH_{relax}) of the samples were measured during the subsequent heating scan from 20 to 180 °C at a rate of 10 °C/min. Such heating and cooling thermal cycle was done at different cooling rates (R_{cool}: 5, 3, or 1 °C/min, see Figure 2). ΔH_{relax} of each sample was obtained from the endothermic peak observed on the

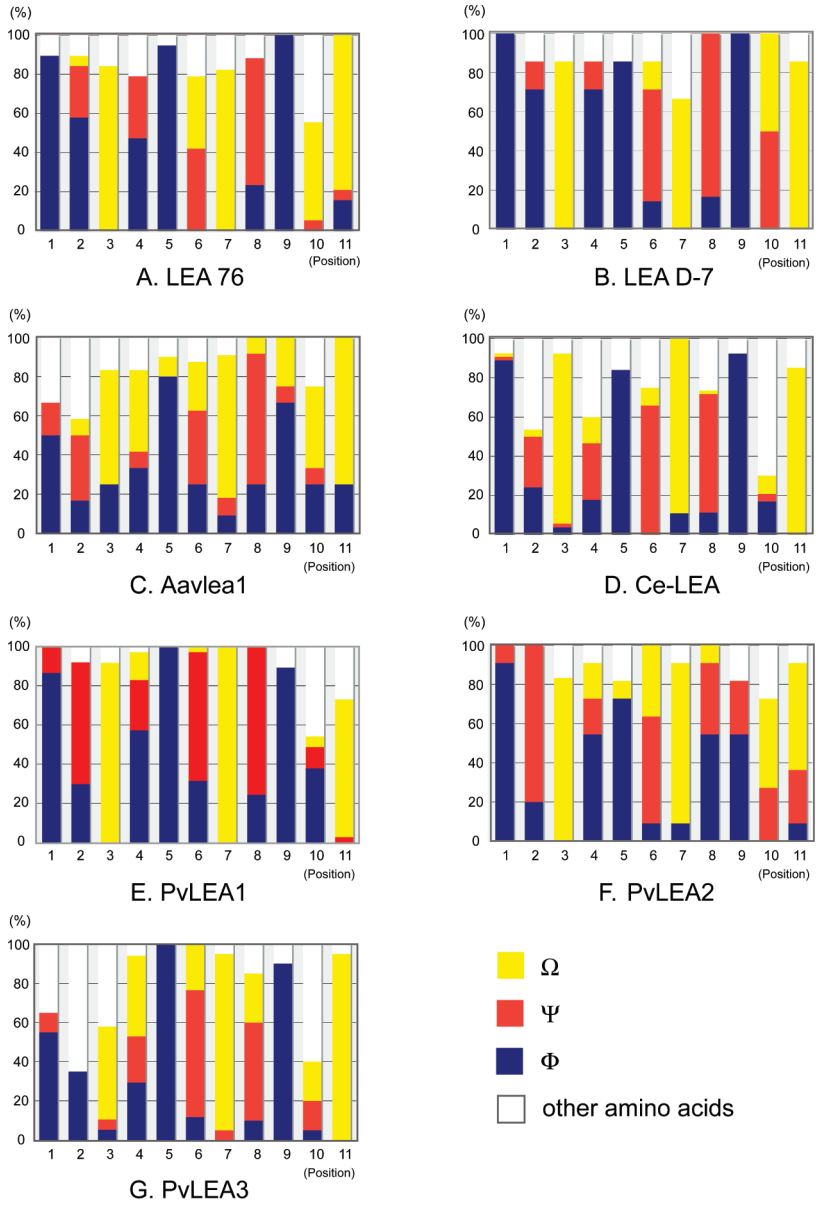

FIGURE 3: Amino acid compositions for each position of the 11-mer repeat unit in the G3LEA proteins. Data are sorted according to Dure's classification for amino acids. (A) and (B) are the results for two kinds of plants, (C) and (D) for two kinds of nematode, and (E)−(G) for three kinds of G3LEA genes of *P. vanderplanki*.

DSC thermogram of each heating scan at 10 °C/min (Figure 2), where the sign of ΔH_{relax} was taken to be minus for the endothermic peak.

RESULTS

Identification of the Consensus 11-mer Amino Acid Motifs of G3LEA Proteins. Figure 3 shows the percentage compositions of the amino acid groups, defined by Dure's report (*18*), for each position in the 11-mer motifs found from the sequence alignment (see Materials and Methods). In LEA 76 and LEA D-7, positions 1, 2, 4, 5, and 9 are occupied predominantly by hydrophobic amino acids (Φ), positions 3, 7, and 11 by negatively charged or amide residues (Ω), and positions 6 and 8 by positively charged residues (Ψ). Thus, the most probable sequence of these plant G3LEA proteins is represented by "ΦΦΩΦΦΨΩΨΦXΩ", where "X" is a nonspecifically conserved amino acid. This is in good agreement with Dure's result, "ΦΦΩXΦΨΩΨΦXΩ", obtained from a more comprehensive survey of plant G3LEA protein genes (*18*). It can therefore be said that our protocol for amino acid sequence analysis (see Materials and Methods) was sufficiently reliable for exploring the 11-mer consensus motif of G3LEA proteins.

The amino acid specificity at positions 2 and 4 is significantly decreased in the 11-mer motifs in AavLEA1 and Ce-LEA, although the overall distributions of the three major groups (Φ, Ω, and Ψ) are very similar to the results for the above plant G3LEA proteins. Intriguingly, position 2 of PvLEA1 and PvLEA2 is predominantly occupied by a positively charged residue, which occurs with a probability of 62% and 80% in the former and latter, respectively. This is in clear contrast to the case of plant G3LEA proteins, where the most frequently occurring residue at position 2 is hydrophobic. In this regard, PvLEA3 is peculiar: its position 2 is predominantly occupied by a residue not belonging to the three major groups (Figure 3G). The predominant residue at position 8 also exhibits a little variation among the three PvLEA proteins. To determine the 11-mer consensus motifs in the PvLEA proteins, we selected the most

Table 1: Amino Acids Found at Each Position of the 11-mer Repeat Units in the G3LEA Proteins[a]

	position in 11-mer repeat unit										
	1	2	3	4	5	6	7	8	9	10	11[a]
LEA 76	≪A≫	< A >	≪Q≫	K	≪T≫	< K >	< E >	≪K≫	≪A≫	< Q >	< E >
	< T >		D	A, T	A	Q	Q	T	T	S	Q[c]
LEA D-7	≪T≫	≪A≫	≪E≫	< A >	≪A≫	K	≪Q≫	≪K≫	≪T≫	E, K	< E >
	< A >			T		R	G			Q, R	Q
Aavlea1	L	R	D	X	≪A≫	< K >	< E >	≪K≫	A	< E >	< E >
			E			A, Q	Q				
Ce-LEA	≪A≫	K	≪D≫	< S >	A	≪K≫	≪D≫	≪K≫	≪A≫	< S >	≪D≫
		A, W		K	V, T		E			G	
PvLEA1	≪A≫	≪K≫	≪D≫	K	≪T≫	≪K≫	≪D≫	≪K≫	≪L≫	< G >	E, D
		A		V, A	A	A	< E >			V	Q
PvLEA2	< A >	≪K≫	≪E≫	T	V	≪K≫	≪D≫	< A >	< A >	E	< E >
			< D >		I	E	E	< K >	K	K	K
PvLEA3	G	< Y >	E	D	< V >	≪K≫	< D >	< K >	A	< P >	≪E≫
	T, V	A	G		I, L	Q	N, E		I, L		D

[a]Probability of finding each amino acid is shown in three ranks: double bracket (≪≫), ≥50%; bracket (< >), <50% and ≥33%; no bracket, <33% and ≥20%.

frequently occurring residue at each position throughout the three PvLEA proteins. According to our sequence analysis, PvLEA1, PvLEA2, and PvLEA3 contained 6, 2, and 3 LEA_4 domains, respectively, each of which comprised 7 or 8 of the 11-mer repeat units (see Materials and Methods). Consequently, the present consensus motif for the PvLEA proteins reflects the amino acid sequence of PvLEA1 most strongly. Taken together, the most probable 11-mer motifs for nematodes and *P. vanderplanki* are given by "ΦXΩXΦΨΩΨΦXΩ" and "ΦΨΩXΦΨΩΨΦXΩ", respectively. Therefore, the amino acid groups at positions 1, 3, 5, 6, 7, 8, 9, and 11 are conserved in all three organisms. In contrast, positions 2 and 4 are less conserved sites, and position 10 has no apparent amino acid specificity in any of the organisms studied here.

Table 1 lists amino acids that occur with high probabilities at each position for each gene, where the probability differences are represented by three ranks using different symbols (see footnote [a] to Table 1). As can be seen from this table, the positively charged residue (Ψ) occurring at positions 6 and 8 is always "K" except for position 6 in the LEA D-7, and thus the conserved residue at these positions in all three organisms is determined as "K". Similarly, the residue at position 2 in the nematode and *P. vanderplanki* LEA proteins can be represented by "K". Among the group Ω residues, "D" and "E" occur most frequently, which suggests that Ω can be represented by "D" or "E". In addition, in most cases Φ can be represented by the simplest residue, "A", except for position 5 of the PvLEA proteins where the most likely residue is "T". Although "T" is treated as a hydrophobic residue in Dure's classification (*18*), it would be unreasonable to replace it by "A". Based on these considerations, the consensus motifs in G3LEA proteins for the three taxa studied here were determined as "AADXAKEKAXE" for plants, "AKDXAKEKAXE" for nematodes, and "AKDXTKEKAXE" for *P. vanderplanki*.

Structure of the Synthesized LEA Models in Solution and Dry States. According to the above analysis, we synthesized four LEA model peptides (PlLEA-22, NeLEA-22, PvLEA-22, PvLEA-44) and a control peptide, whose amino acid sequences are shown in Figure 4. In these models, "G" was employed as "X" because it has no specific effect on the structural property of the peptide backbones. The control peptide has an amino acid composition identical to that of PvLEA-22, but the sequence has been altered so that it does not correspond to any known 11-mer motif.

		1	2	3	4	5	6	7	8	9	10	11	
PvLEA-44	H_2N-(	A	K	D	G	T	K	E	K	A	G	E	)$_4$-$CONH_2$
PvLEA-22	H_2N-(	A	K	D	G	T	K	E	K	A	G	E	)$_2$-$CONH_2$
NeLEA-22	H_2N-(	A	K	D	G	A	K	E	K	A	G	E	)$_2$-$CONH_2$
PlLEA-22	H_2N-(	A	A	D	G	A	K	E	K	A	G	E	)$_2$-$CONH_2$
control	H_2N-(	A	K	E	K	E	G	T	D	K	A	G	
		G	A	K	D	T	G	E	K	E	K	A	) -$CONH_2$

FIGURE 4: Amino acid sequences of the chemically synthesized LEA models (PvLEA-44, PvLEA-22, NeLEA-22, PlLEA-22) and the control peptide. The amino acid composition of the control is identical to that of PvLEA-22.

Panels A and B of Figure 5 show the amide I and amide II regions of the FTIR spectra for PlLEA-22, NeLEA-22, PvLEA-22, PvLEA-44, and the control in D_2O and their second-derivative spectra. It can be seen that all spectra have two major peaks in a region from 1600 to 1700 cm^{-1}. Their peak positions are accurately determined to be 1642 and 1674 cm^{-1} from the second-derivative spectra. By reference to the literature (*39*, *40*), these peaks are assigned to random coils and β-turns, respectively. Another characteristic feature of Figure 5A is that there is no apparent peak in the amide II region (1520−1590 cm^{-1}), which implies that almost all of the amide protons were exchanged for deuterium. This is also a characteristic of a disordered structure (*41*). Thus, the FTIR spectra indicate that all four LEA models together with the control peptide are unstructured in D_2O.

Figure 5C shows the amide I region of the FTIR spectra and their second-derivative spectra for the five peptides in the dry state. Compared with Figure 5A, the amide I bands are significantly broadened, especially in the LEA models. The second-derivative spectra, however, showed that the amide I band of the LEA models could be resolved into several peaks and that the corresponding band in the control involved only two peaks located at almost the same positions as those observed for the hydrated sample. These findings suggest that the LEA models

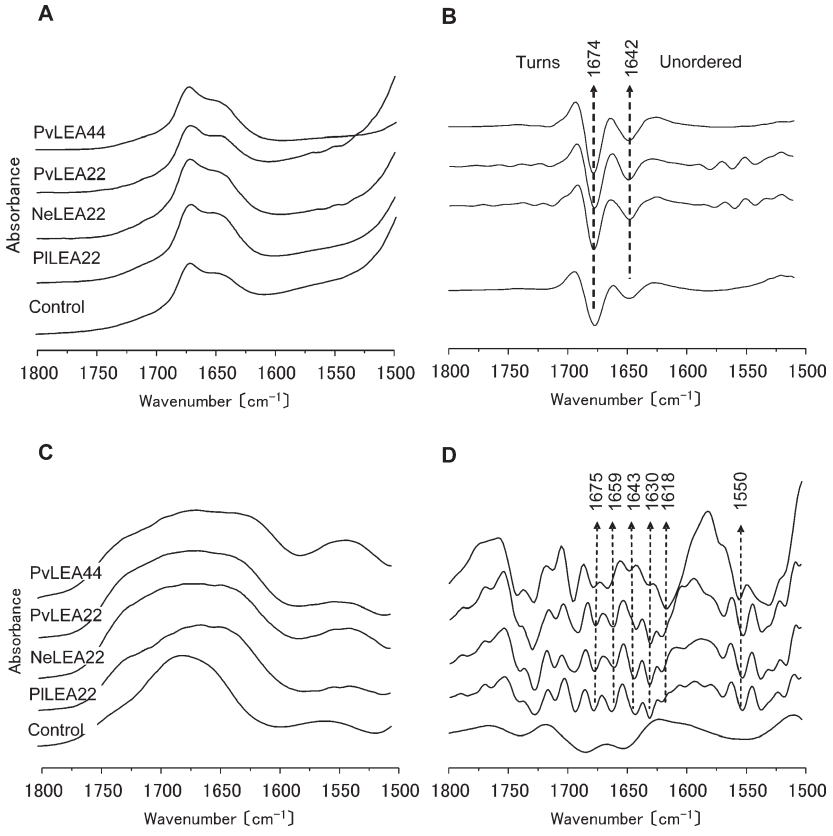

FIGURE 5: Amide I and amide II regions of FTIR spectra for the LEA models (PvLEA-44, PvLEA-22, NeLEA-22, PlLEA-22) and the control peptide in D_2O solution (A) and in the dry state (C). (B) and (D) are the corresponding second-derivative spectra.

Table 2: Band Positions and Areas of the Amide I Spectra of the Investigated LEA Models and Representative Coiled-Coil Proteins

	band 1 (cm^{-1})[a]	band 2 (cm^{-1})[a]	band 3 (cm^{-1})[a]	band 4 (cm^{-1})[a]	band 5 (cm^{-1})[a]
PvLEA-44	1614 (19.4);	1630 (30.3);	1646 (20.7);	1662 (12.6);	1678 (17.0);
PvLEA-22	1618 (17.8);	1630 (22.5);	1643 (15.2);	1659 (19.7);	1674 (24.8);
NeLEA-22	1619 (25.1);	1630 (7.81);	1640 (7.2);	1659 (45.8);	1675 (14.2);
PlLEA-22	1619 (11.1);	1630 (24.7);	1640 (25.1);	1660 (24.8);	1675 (14.3);
tropomyosin[b]	1607 (7.9);	1626 (24.9);	1639 (33.0);	1652 (23.9);	1668 (10.3);
COMP rod[b]	1614 (1.2);	1631 (25.0);	1644 (17.9);	1652 (47.9);	1673 (8.0);
fibritin[b]	1610 (6.3);	1631 (21.2);	1641 (20.6);	1651 (35.0);	1670 (16.7);

[a]Relative band areas are written in parentheses. [b]Data were cited from ref *43*.

underwent dramatic conformational changes on going from the aqueous to the dried state, whereas the structure of the control peptide was almost unchanged on drying.

At this stage, it is of interest to examine what structure(s) are formed in the dried LEA models. The peak absorbing at 1659 cm^{-1} can be assigned to α-helical structures (*39*, *40*). The peak at around 1550 cm^{-1}, corresponding to the amide II band, also shows the presence of an α-helical structure, whereas the control gave spectra characteristic of a disordered structure (1535 cm^{-1}) (*39*, *40*). According to Heimburg et al.(*42*, *43*), multistranded coiled coils have unique vibrational spectra with at least three separable bands instead of the single band of a classical α-helix in the amide I region. Table 2 summarizes the peak positions of the amide I bands of well-known multistranded coiled-coil proteins and the LEA models studied here. Intriguingly, peak positions 1618, 1630, 1643, and 1674 cm^{-1} obtained for the LEA models (see the second derivative spectra of Figure 5D) are in good agreement with the literature values obtained for α-helical coiled coils.

In addition to the above peaks, there are also clear peaks around 1618 and 1690 cm^{-1}. The simultaneous appearance of these peaks is characteristic of intermolecular β-sheet formation (*39*, *40*). This result implies that some fraction of the LEA model peptides may have aggregated on dehydration. The peaks assignable to the intermolecular β-sheet have been also observed for dehydrated native G3LEA proteins from either nematode (*26*) or pea seed mitochondria (*27*), together with five peaks observed for α-helical coiled-coil proteins (*43*). It is of great surprise that the current short peptides can reproduce well the structural features of the parent G3LEA protein.

On rehydration of the dried LEA models with D_2O, the two original peaks again appeared around 1642 and 1674 cm^{-1}, and the peak around 1550 cm^{-1} disappeared (data not shown). In other words, the original solution spectra were recovered and the LEA models transformed to random coils on rehydration. These results indicate that the synthesized LEA models of the repeated 11-mer units of G3LEA proteins can reversibly transform

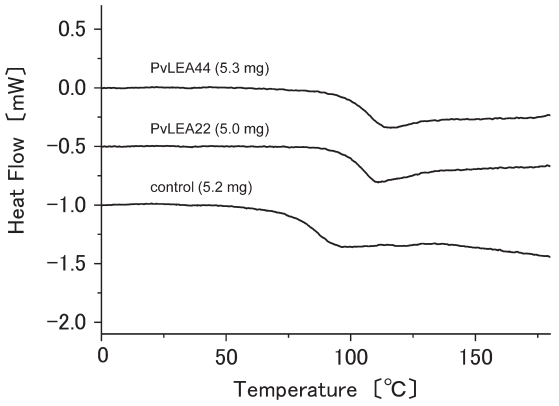

FIGURE 6: DSC thermograms for PvLEA-44, PvLEA-22, and the control peptide in the dry state. The amount of sample used is given in parentheses.

between random coils and α-helical coiled coils in response to the change of water activity.

Glass Transition and Enthalpy Relaxation of the LEA Models in the Dry State. Figure 6 shows the heat absorption of dried PvLEA-22, PvLEA-44, and the control peptide in the second DSC heating scan. All of the peptides exhibited a clear baseline shift in a stepwise manner, indicating the occurrence of a glass transition. PvLEA-22 and PvLEA-44 exhibited almost the same glass transition temperatures (T_g): onset, middle, and endset temperatures were 99, 102, and 108 °C, respectively. This means that these LEA models are in a glassy state at < 99 °C and in a rubbery state at > 108 °C. In contrast, the T_g of the control peptide (onset, 79 °C; middle, 84 °C; endset, 91 °C) was about 18 °C lower than those of PvLEA-44 and PvLEA-22. Here it may be worth noting that little or no change was observed for both FTIR spectra of PvLEA-22 and the control in a temperature range from 30 to 180 °C (data not shown). That is, their molecular structures underwent no apparent change during the glass transition. This is consistent with the finding that no thermal events were observed except for glass transition and/or its enthalpy relaxation (in the next paragraph) on DSC thermograms obtained. Taken together with the structural information given in the previous section, the transformation into α-helical coiled coil seems to be associated with facilitated vitrification of the PvLEA models, although there may be more or less of the synergetic contribution from intermolecular β-sheet formation.

Figure 7A shows the DSC heating thermograms for dried PvLEA-22, which previously experienced different cooling rates, R_{cool} (see Figure 2). An endothermic peak near T_g, which corresponds to the enthalpy relaxation (ΔH_{relax}) of the glassy matrix, was observed for each thermogram. With decreasing cooling rate, peak area increased, indicating an increasing enthalpy of relaxation. DSC heating thermograms for dried control peptide also showed similar behavior (data not shown). In both PvLEA-22 and the control, there is good linearity between ln R_{cool} and ΔH_{relax} (Figure 7B). Interestingly, ΔH_{relax} of PvLEA-22 was smaller than that of the control at each of the cooling rates examined, and the slope of the line is larger in PvLEA-22 than in the control. These findings suggest that the glassy matrix formed from α-helical coiled-coil chains concomitant with intermolecular β-sheet (i.e., PvLEA-22) is kinetically more stable than that of a random coil (i.e., the control peptide).

Structural and Thermodynamic Properties of LEA Models in the Presence of Trehalose. To examine the structure of dried PvLEA-22 in the presence of trehalose, we dried mixtures

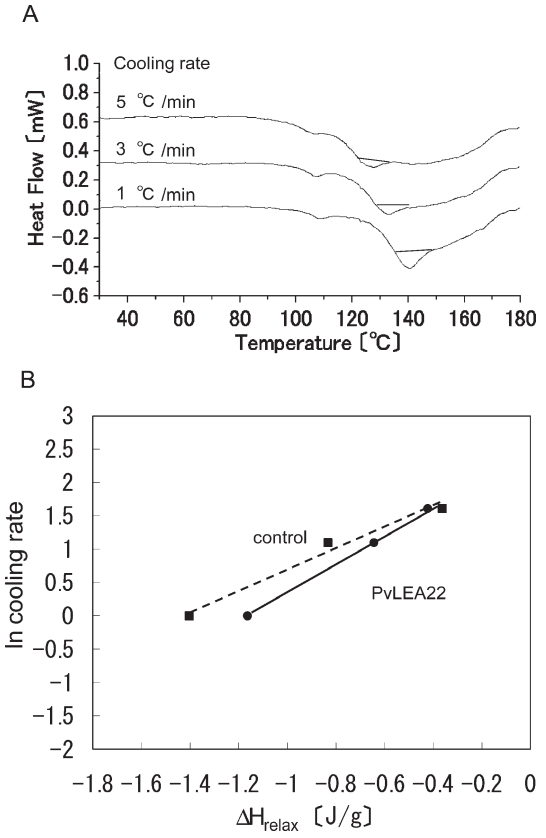

FIGURE 7: (A) Cooling rate dependence of DSC heating thermograms for dried PvLEA-22 and (B) logarithm of cooling rate versus enthalpy relaxation (ΔH_{relax}) for PvLEA-22 (solid line) and for the control peptide (dashed line).

(with molar ratios of PvLEA-22:trehalose in the range 1:1−1:5) in the same way as for the pure peptide: a droplet (5 μL) of the mixture dissolved in D_2O was placed in a desiccator (RH 5%) for 24 h at 25 °C (see Materials and Methods). A similar method was followed with control peptide/trehalose mixtures.

Figure 8 depicts the amide I and amide II regions of the FTIR spectra for the dried PvLEA-22/trehalose mixtures. Similarly to the trehalose-free sample, five characteristic peaks were observed in the amide I region, and the amide II showed characteristics of an α-helical structure (1550 cm^{-1}). This suggests that the coiled-coil formation of PvLEA-22 is not greatly disturbed by the presence of trehalose in molar ratios up to 1:5. Similarly, trehalose exerted no apparent influence on the structure of the control peptide: in this case the peptide remained unstructured (data not shown).

Next, we examined the properties of glasses of the above PvLEA-22/trehalose mixtures. In this case, DSC measurements were not necessary because their glass transition behavior can be examined by monitoring the OH vibration band of the sugar using FTIR spectroscopy (*28*). To confirm the reliability of this method, we compared the glass transition temperatures obtained from FTIR and DSC measurements for anhydrous glassy trehalose, which was prepared as follows: trehalose dihydrate was heated to 140 °C, followed by rapid cooling to room temperature. Figure 9 (top) shows the temperature dependence of the OH stretching vibration peak of such a sample. The inflection point, indicating the occurrence of a glass transition, is observed at 112 °C, in good agreement with the result (117 °C) from DSC measurements (data not shown).

The middle and bottom panels of Figure 9 show the temperature dependence of the maximal peak position (ν_{high} cm^{-1}) of the

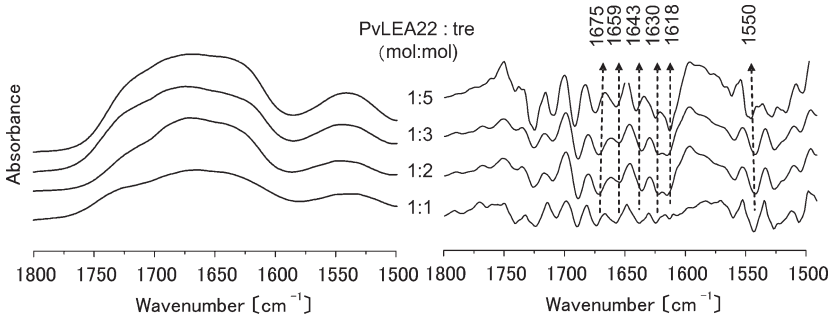

FIGURE 8: Amide I and amide II regions of FTIR spectra for PvLEA-22 in the presence of trehalose in the dry state.

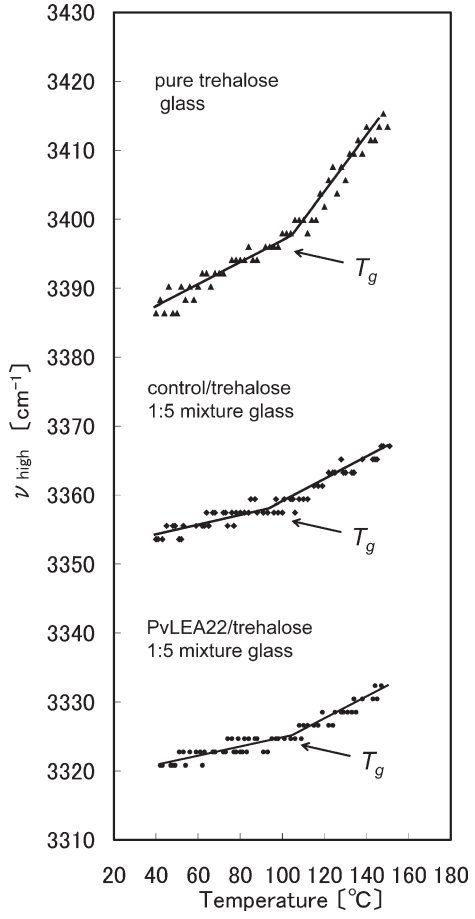

FIGURE 9: Temperature dependence of the maximal peak position of the OH stretching band observed for pure trehalose glass (top), trehalose/control 5:1 mixture, and trehalose/PvLEA-22 5:1 mixture in the dry state.

OH stretching vibration region for the dried PvLEA-22:trehalose and control peptide:trehalose mixtures. A clear inflection point (T_g) was observed at about 103 and 96 °C for the PvLEA-22:trehalose (1:5) and control peptide:trehalose (1:5), respectively. It should be noted that the T_g of the former mixture is nearly equal to that of pure PvLEA-22 obtained from the DSC measurements. The fact that the T_g of the PvLEA-22/trehalose mixture is higher than that of the control peptide/trehalose mixture implies that the presence of the PvLEA-22 peptide that is capable of transforming into a coiled-coil conformation results in a more stable trehalose glass than that formed with the control, randomly coiled peptide. Other features to be noted in Figure 9 are as follows: (1) the ν_{high} of the PvLEA-22:trehalose (1:5) glass was shifted by about 40 cm^{-1} to the lower wavenumber side compared with that of the control peptide:trehalose (1:5) glass, and (2) the slope of the temperature-dependent plot is less steep in the mixture samples than the pure trehalose glass. Finding 1 shows that the hydrogen-bonding network in the glassy state is strengthened in the former mixture compared to the latter. Combining findings 1 and 2, it can be said that the glassy matrix of trehalose is strengthened by the addition of the peptides, and this effect is larger with the G3LEA model peptide than with the control.

DISCUSSION

In this study, we determined the consensus sequence of the 11-mer repeat motifs of G3LEA proteins from three anhydrobiotic organisms. As shown in Table 1, positions 4 and 10 exhibited no apparent amino acid specificity, consistent with Dure's results for plants (*18*). In addition, little variation was found at positions 2 and 5, whose amino acids are (K, T), (K, A), and (A, A) for PvLEA, NeLEA, and PlLEA, respectively (see Figure 3). As can be seen from the α-helical wheel (Figure 1), the residues at positions 4 and 10 are embedded in the wide hydrophilic stripe composed of many charged residues. Thus, it is likely that amino acid variations at these positions have little influence on the structural property of the polypeptide chain. On the other hand, position 2 is located at the boundary between the hydrophilic stripe and the narrow hydrophobic one, and thereby the amino acid selection at this position, i.e., polar or apolar residue, might exert a subtle influence on the amphiphilic character. Similarly, the selection of T instead of A at position 5 in PvLEA might result in a decrease in hydrophobicity of the narrow stripe. The effects of amino acid changes at these positions will be discussed below.

According to previous reports, G3LEA proteins were found to adopt random coil structures in solution (*26*, *44*−*46*) and to transform to α-helices or α-helical coiled coils in the dehydrated state, although they became unstructured again on rehydration (*26*−*28*, *45*, *47*). However, these studies, focusing on the native proteins alone, have provided no information on what part of the primary sequence is responsible for such an intriguing structural property. The present FTIR results indicated that all of the LEA models undergo a structural transformation to α-helical coiled coils upon dehydration and return to random coil upon rehydration (Figure 5). In contrast, no apparent structural changes were observed for the control peptide, which remained unstructured irrespective of water content. These results clearly indicate that the dehydration-induced coiled-coil formation represents the intrinsic nature of the peculiar 11-mer repeat sequences commonly found in G3LEA proteins. It is likely therefore that the 11-mer motifs play an essential role in driving the coiled-coil formation of a full-length G3LEA protein, although the structural properties of the residual nonrepeating regions are currently unknown.

It was confirmed from the FTIR spectra that in the dry state some fraction of the present LEA peptides formed β-sheet structure, being consistent with the results for the native G3LEA proteins (*26*, *27*). However, it is currently doubtful whether or not the β-sheet structure really acts as a functional unit in the LEA proteins, because such a secondary structure is often formed in the misfolded state of proteins (*48*). We will therefore focus our attention only upon the functional role of coiled-coil structure in the following discussion.

In general, a coiled coil is characterized by several geometrical parameters: the number of helices it contains, the crossing angle of helices, superhelical pitch, the radius of curvature, and the mutual orientations of helices (parallel or antiparallel). Among these, the difference in superhelical pitch is known to be reflected in the FTIR spectra in the amide I region (*43*, *44*). Namely, the spectrum of a dimeric coiled coil exhibits a large deviation from a normal α-helical spectrum as a result of relatively short superhelical pitch (or large geometrical distortion of the constitutive helices), while the spectral anomalies of trimeric and pentameric coiled coils are less pronounced. As shown in Table 2, in the case of a trimeric coiled-coil-like COMP rod, the largest contribution to the amide I band comes from band 4 located at 1652 cm^{-1} (Table 2), very close to a normal α-helical band position at 1650−1653 cm^{-1}. A similar coincidence of wavenumbers is observed with a pentameric coiled-coil-like fibritin. In contrast, in the case of a dimeric coiled-coil-like tropomyosin, the maximal contribution comes from band 3, meaning a low wavenumber shift of the spectral maximum of the overall amide I band. On the basis of these literature data, we consider the results for the LEA models given in Table 2. For NeLEA-22, the result is similar to that of the COMP rod in that band 4 is the largest contributor, although the relative ratios of bands 1 and 2 are reversed between them. This suggests that the coiled coil of NeLEA-22 has a long superhelical pitch, consistent with the previous report by Goyal et al. (*26*), who inferred that the superhelical assembly of the native nematode LEA protein may originate from the lateral association of helices in a straight manner without any twisting. In the cases of PvLEA-44 and PvLEA-22, the weight of band 4 significantly decreases as for tropomyosin, and hence they are expected to take nearly dimeric coiled coils. We cannot find any simple relationship between the amino acid compositions at positions 2 and 5 and the geometrical differences of the resulting coiled coil.

It has been reported that a G3LEA protein (AavLEA1) from an anhydrobiotic nematode can prevent desiccation-induced aggregation of a wide range of other proteins both *in vitro* and *in vivo* without the requirement for any other desiccation protectant like a sugar (*23*, *49*). Some other LEA proteins are known to have a function of maintaining membrane integrity in the dry state (*23*, *27*). To understand why LEA proteins alone can act as desiccation protectants, it is necessary to investigate not only their structural properties but also their thermal properties in the dry state, especially glass transition properties. Such data have not been reported so far, probably because thermodynamic measurements require a relatively large amount of protein sample. In this study, use of chemically synthesized model peptides instead of native proteins enabled us to prepare a sufficient amount of sample for direct DSC analysis. Consequently, we obtained evidence that they form highly stable glasses at room temperature in the dry state: the T_g of both PvLEA-22 and PvLEA-44 was observed at 102 °C. The control peptide also exhibited a high glass transition temperature (84 °C).

The T_g values of the trehalose/peptide mixtures are lower than that of dehydrated pure trehalose, 112 °C (Figure 9), which is nearly equal to the T_g value of completely water-free glassy trehalose (*50*, *51*). As described in the Materials and Methods section, the pure trehalose sample was obtained by heating the trehalose dihydrate crystal to 140 °C and subsequent rapid cooling, whereas the trehalose/peptide mixture samples were obtained through dehydration in a desiccator (RH 5%): their final residual water content was ca. 2 wt %. Thus, the T_g data in Figure 9 should not be compared directly with those of the trehalose/peptide mixtures. Instead, we estimated the T_g value of pure glassy trehalose with the water content of 2 wt % from the experimentally parametrized Gordon−Taylor equation (*52*). As a result, the value of 86 °C (as onset of the glass transition) was obtained. It is therefore likely that the T_g values of the trehalose/peptide mixtures are higher than that of pure trehalose at a given equal water content.

When the physical stability of vitrified material in itself is considered, the enthalpy relaxation is an important phenomenon (*38*, *51*). Here we successfully observed the enthalpy relaxation of these peptides by using a method recently developed by Kawai et al. (*38*), allowing measurements of enthalpy relaxation for a limited amount of sample. As shown in Figure 7B, the value of the enthalpy relaxation is always smaller in PvLEA-22 than in the control when it is compared for the same cooling rate. This clearly indicates that the former glass is more stable than the latter. In general, the relaxation process is quantified by the activation energy for molecular rearrangements leading to energetically more relaxed states. Such molecular rearrangements are caused by cooperative molecular motions. The higher the cooperativity, the higher the activation energy. The results of Figure 7B can therefore be interpreted as intermolecular interactions leading to coiled-coil formation bringing about high cooperative motions, resulting in a high activation energy, in other words, a low enthalpy relaxation rate. Taken together, the structural transformation to a coiled coil not only facilitates vitrification of the polypeptides themselves but also contributes to the production of a more stable glass.

The above arguments are based only on the experimental data for PvLEA-22 and PvLEA-44, and it is of interest to know the extent to which the subtle differences in the 11-mer repeat sequences influence the property of the resulting glassy matrix. For this purpose, we attempted to predict the T_g values of the other LEA models synthesized here based on a theory for calculating the glass transition temperature of a protein. According to a report by Matveev et al.(*53*), the T_g of a protein is calculated by the equation:

$$T_g^{-1} = \sum_{i=1}^{20} \phi_i T_{g,i}^{-1} \quad (1)$$

where

$$\phi_i = \frac{n_i \Delta V_i}{\sum_{i=1}^{20} n_i \Delta V_i} \quad (2)$$

ΔV_i is the van der Waals volume of the ith amino acid residue, n_i is the number of amino acid residues of the ith type per one protein molecule, and $T_{g,i}$ is the partial increment of the T_g by the ith residue. Table 3 lists the values of ΔV_i and $T_{g,i}$ necessary for calculating the T_g values of the three LEA models. To confirm the

Table 3: Results of the Calculated T_g Values for PvLEA, NeLEA, and PlLEA

			PvLEA		NeLEA		PlLEA	
aa	$T_{g,i}$[a]	ΔV_i[a]	no. of aa	φ_i[b]	no. of aa	φ_i	no. of aa	φ_i
G	599	47.3	2	0.1005	2	0.1032	2	0.1096
A	621	64.4	2	0.1369	3	0.2108	4	0.2985
T	321	88.9	1	0.0945	0	0	0	0
D	672	80.1	1	0.0851	1	0.0874	1	0.0928
E	487	97.2	2	0.2066	2	0.2121	2	0.2253

[a]The physical meanings of $T_{g,i}$ and ΔV_i are described in the text. These data were cited from ref *49*. [b]See eq 2 in the text.

reliability of this theory, we first calculated the T_g of the PvLEA models. Since the above equations depend only on the amino acid composition of a given protein and not on its molecular weight, they gave the same T_g values of 98 °C for PvLEA-22 and PvLEA-44. This is in a good agreement with the experimental value of 102 °C (middle temperature), considering that the glass transition occurs within a temperature range of about 10 °C from onset to endset. Table 3 also lists the T_g values calculated for NeLEA and PlLEA, which are higher than that of PvLEA by 47 and 63 °C, respectively, giving the relative order of the T_g values for the three LEA models as PvLEA < NeLEA < PlLEA. This result can be clearly explained from the difference in the amino acid compositions at positions 2 and 5. As shown in Table 3, T and K have smaller $T_{g,i}$ and larger ΔV_i values compared with the other residues, and thereby their contributions to the final T_g value are relatively smaller as can be seen from eqs 1 and 2. Therefore, PvLEA has the lowest T_g among the three LEA proteins. Comparing PvLEA to NeLEA, T at position 5 is replaced by A, leading to an increase of T_g. Similarly, an increase in T_g from NeLEA to PlLEA can be explained by mutation from K to A at position 2. It is unclear only from the present *in vitro* study what biological significance is given to these differences in T_g. It may be said, however, that the T_g of the G3LEA proteins are significantly higher than environmental temperatures at which anhydrobiotic organisms live: for example, the maximal temperature of rock surfaces where desiccated larvae of *P. vanderplanki* are placed is as high as 60 °C. Therefore, dried LEA proteins alone should act as a good desiccation protectant if they act through a vitrification mechanism in a similar way to sugars like trehalose and sucrose.

Many anhydrobiotic organisms accumulate trehalose or sucrose together with G3LEA proteins under desiccation stress (*25*, *26*, *28*, *30*). The present FTIR results, mainly obtained for PvLEA-22/trehalose mixtures, provided invaluable information about what role the LEA proteins play in such a situation (Figure 8). Dried PvLEA-22 maintains a coiled-coil structure even in the presence of an excess of trehalose (Figure 8); moreover, the dried PvLEA-22/trehalose (1:5) mixture vitrifies at room temperature (Figure 9). Interestingly, its T_g is 103 °C, very close to that of pure PvLEA-22. When PvLEA-22 was added to trehalose, only one inflection point (T_g) was observed in the temperature-dependent shift of the OH band. This suggests that the resulting glassy matrix is just the binary mixture of trehalose and PvLEA-22. Furthermore, the T_g of the PvLEA-22/trehalose (1:5) mixture is higher than that of the control peptide/trehalose (1:5) mixture by 7 °C. It is therefore inferred that coiled-coil incorporation results in a glassy matrix with a higher T_g. This is possibly because PvLEA-22 reinforces the hydrogen bond network in trehalose glass with a stronger effect than the control peptide, as indicated by the comparison of the OH band positions and the slope of the temperature dependent shift (Figure 9). The decrease in the slope means an increase in the activation energy for hydrogen bond rearrangements around the glass transition temperature, and therefore the addition of the LEA peptide results in a decrease in enthalpy relaxation rate of the glassy matrix.

The above findings support the steel-reinforced concrete model proposed by Goyal et al. (*26*). That is, G3LEA proteins, particularly their repeated 11-mer amino acid moieties, and trehalose (or sucrose) could synergistically stabilize proteins, macromolecular and cellular structures, in a manner analogous to steel-reinforced concrete, where the G3LEA proteins folded into coiled-coil structures and vitrified trehalose act as steel and concrete, respectively. This model is helpful for interpreting the glassy property of real anhydrobiotic organisms. Recently, we found that it was inexplicable with only two components, trehalose and water, how the glassy property of larvae of *P. vanderplanki* persist in their successful anhydrobiotic states at different moisture contents: observed glass transition temperatures became higher than expected for a binary trehalose:water mixture as their water content gradually increased (*31*). This result could be understood if G3LEA proteins, such as PvLEA1, PvLEA2, and PvLEA3, are able to strengthen the glassy matrix of the endogenous trehalose, as indicated by increased glass transition temperatures relative to those of pure trehalose.

Finally, we discuss whether the short peptides synthesized here have the potential to act as desiccation protectants in their own right. In this regard, the work by Honjoh et al. is very informative (*54*). They prepared five kinds of LEA model peptides, which were composed of the 11-mer amino acid motif found in G3LEA proteins from a freeze-tolerant algae *Chlorella vulgaris* C-27, and measured the cryoprotective activity of those peptides. It was shown that the activity declined with decreasing number of 11-mer repeat units involved; a 22-mer was the minimal length for apparent activity. The functional aspects of the 22-mer and 44-mer models synthesized here, such as protection against dehydration-induced protein aggregation, are now under investigation in our laboratory.

CONCLUSION

In this study, we obtained answers to several questions concerning the intrinsic nature of the peculiar 11-mer repeat units found in G3LEA proteins. First, our FTIR spectroscopic measurements demonstrate that all LEA models underwent reversible structural changes between random coils and α-helical coiled coils in response to water activity. Thus, the peculiar structural behavior of some native G3LEA proteins found in previous studies (*26*−*28*) was reproduced by the short peptides synthesized here, which implies that the 11-mer repeat units might be responsible for the structural transformation of full-length G3LEA proteins. Second, our DSC data provide the first evidence that the 11-mer repeat units in G3LEA proteins themselves can form a stable glassy matrix with a high T_g on dehydration. Furthermore, these units act as reinforcements for the glassy matrix of the disaccharide, trehalose. On the basis of these results, it can be inferred that the coiled-coil assembly of G3LEA proteins acts not only as mechanical support for the intracellular matrix but also as a thermal stabilizer of biological glasses.

ACKNOWLEDGMENT

We thank Dr. Alan Tunnacliffe (University of Cambridge) for helpful comments on the manuscript. We gratefully acknowledge Prof. Yoshio Inoue (Tokyo Institute of Technology) for use of the DSC instrument.

REFERENCES

1. Dure, L., III, Greenway, S. C., and Galau, G. A. (1981) Developmental biochemistry of cottonseed embryogenesis and germination: Changing messenger ribonucleic acid populations as shown by in vitro and in vivo protein synthesis. *Biochemistry 20*, 4162–4168.
2. Grzelczak, Z. F., Sattolo, M. H., Hanley-Bowdoin, L. K., Kennedy, T. D., and Lane, B. G. (1982) Synthesis and turnover of proteins and mRNA in germinating wheat embryos. *Can. J. Biochem. 60*, 389–397.
3. Galau, G. A., Hughes, D. W., and Dure, L., III (1986) Abscisic acid induction of cloned cotton late embryogenesis-abundant (Lea) mRNAs. *Plant Mol. Biol. 7*, 155–170.
4. Hughes, D. W., and Galau, G. A. (1989) Temporally modular gene expression during cotyledon development. *Genes Dev. 3*, 358–369.
5. Roberts, J. K., DeSimone, N. A., Lingle, W. L., and Dure, L., III (1993) Cellular concentrations and uniformity of cell-type accumulation of two LEA proteins in cotton embryos. *Plant Cell 5*, 769–780.
6. Bray, E. A. (1993) Molecular responses to water deficit. *Plant Physiol. 103*, 1035–1040.
7. Bray, E. A. (1997) Plant responses to water deficit. *Trends Plant Sci. 2*, 48–54.
8. Cuming, A. (1999) in Seed Proteins (Shewry, P. R., and Casey, R., Eds.) pp 753−780, Kluwer Academic Publishers, Dordrecht, The Netherlands.
9. Keilin, D. (1959) The Leeuwenhoek lecture: The problem of anabiosis or latent life: History and current concept. *Proc. R. Soc. London 150B*, 149–191.
10. Ried, J. L., and Walker-Simmons, M. K. (1993) Group 3 late embryogenesis abundant proteins in desiccation-tolerant seedlings of wheat (*Triticum aestivum* L.). *Plant Physiol. 102*, 125–131.
11. Blackman, S. A., Obendorf, R. L., and Leopold, A. C. (1995) Desiccation tolerance in developing soybean seeds: The role of stress proteins. *Physiol. Plant. 93*, 630–638.
12. Joh, T., Honjoh, K., Yoshimoto, M., Funabashi, J., Miyamoto, T., and Hatano, S. (1995) Molecular cloning and expression of hardening-induced genes in *Chlorella vulgaris* C-27: The most abundant clone encodes a late embryogenesis abundant protein. *Plant Cell Physiol. 36*, 85–93.
13. Ingram, J., and Bartels, D. (1996) The molecular basis of dehydration tolerance in plants. *Annu. Rev. Plant Physiol. Plant Mol. Biol. 47*, 377–403.
14. Battista, J. R., Park, M.-J., and McLemore, A. E. (2001) Inactivation of two homologues of proteins Presumed to be involved in the desiccation tolerance of plants sensitizes *Deinococcus radiodurans* R1 to desiccation. *Cryobiology 43*, 133–139.
15. Bartels, D., and Salamini, F. (2001) Desiccation tolerance in the resurrection plant *Craterostigma plantagineum*. A contribution to the study of drought tolerance at the molecular level. *Plant Physiol. 127*, 1346–1353.
16. Dure, L., III, Crouch, M., Harada, J., Ho, T. H. D., Mundy, J., Quatrano, R., Thomas, T., and Sung, Z. R. (1989) Common amino acid sequence domains among the LEA proteins of higher plants. *Plant Mol. Biol. 12*, 475–486.
17. Dure, L., III (1993) A repeating 11-mer amino acid motif and plant desiccation. *Plant J. 3*, 363–369.
18. Dure, L., III (2001) Occurrence of a repeating 11-mer amino acid sequence motif in diverse organisms. *Protein Pept. Lett. 8*, 115–122.
19. Browne, J., Tunnacliffe, A., and Burnell, A. (2002) Anhydrobiosis: Plant desiccation gene found in a nematode. *Nature 416*, 38.
20. Gal, T. Z., Glazer, I., and Koltai, H. (2003) Differentail gene expression during desiccation stress in the insect-killing nematode *Steinernema feltlae* IS-6. *J. Parasitol. 89*, 761–766.
21. Gal, T. Z., Glazer, I., and Koltai, H. (2004) An LEA group 3 family member is involved in survival of *C. elegans* during exposure to stress. *FEBS Lett. 577*, 21–26.
22. Tunnacliffe, A., Lapinski, J., and McGee, B. (2005) A putative LEA protein, but no trehalose, is present in anhydrobiotic bdelloid rotifers. *Hydrobiologia 546*, 315–321.
23. Pouchkina-Stantcheva, N. N., McGee, B. M., Boschetti, C., Tolleter, D., Chakrabortee, S., Popova, A. V., Meersman, F., Macherel, D., Hincha, D. K., and Tunnacliffe, A. (2007) Functional divergence of former alleles in an ancient asexual invertebrate. *Science 318*, 268–271.
24. Browne, J. A., Dolan, K. M., Tyson, T., Goyal, K., Tunnacliffe, A., and Burnell, A. M. (2004) Dehydration-specific induction of hydrophilic protein genes in the anhydrobiotic nematode *Aphelenchus avenae*. *Eukaryot. Cell 3*, 966–975.
25. Kikawada, T., Nakahara, Y., Kanamori, Y., Iwata, K., Watanabe, M., McGee, B., Tunnacliffe, A., and Okuda, T. (2006) Dehydration-induced expression of LEA proteins in an anhydrobiotic chironomid. *Biochem. Biophys. Res. Commun. 348*, 56–61.
26. Goyal, K., Tisi, L., Basran, A., Browne, J., Burnell, A., Zurdo, J., and Tunnacliffe, A. (2003) Transition from natively unfolded to folded state induced by desiccation in an anhydrobiotic nematode protein. *J. Biol. Chem. 278*, 12977–12984.
27. Tolleter, D., Jaquinod, M., Mangavel, C., Passirani, C., Saulnier, P., Manon, S., Teyssier, E., Payet, N., Avelange-Macherel, M. H., and Macherel, D. (2007) Structure and function of a mitochondrial late embryogenesis abundant protein are revealed by desiccation. *Plant Cell 19*, 1580–1589.
28. Wolkers, W. F., McReady, S., Brandt, W. F., Lindsey, G. G., and Hoekstra, F. A. (2001) Isolation and characterization of a D-7 LEA protein from pollen that stabilizes glasses in vitro. *Biochim. Biophys. Acta 1544*, 196–206.
29. Tunnacliffe, A., and Lapinski, J. (2003) Resurrecting Van Leeuwenhoek's rotifers: A reappraisal of the role of disaccharides in anhydrobiosis. *Philos. Trans. R. Soc. London, Ser. B 358*, 1755–1771.
30. Watanabe, M., Kikawada, T., Minagawa, N., Yukuhiro, F., and Okuda, T. (2002) Mechanism allowing an insect to survive complete dehydration and extreme temperatures. *J. Exp. Biol. 205*, 2799–2802.
31. Sakurai, M., Furuki, T., Akao, K., Tanaka, D., Nakahara, Y., Kikawada, T., Watanabe, M., and Okuda, T. (2008) Vitrification is essential for anhydrobiosis in an African chironomid, *Polypedilum vanderplanki*. *Proc. Natl. Acad. Sci. U.S.A. 105*, 5093–5098.
32. Baker, J., Steele, C., and Dure, L., III (1988) Sequence and characterization of 6 LEA proteins and their genes from cotton. *Plant Mol. Biol. 11*, 277–291.
33. Harada, J. J., DeLisle, A. J., Baden, C. S., and Crouch, M. L. (1989) Unusual sequence of an abscisic acid-inducible mRNA which accumulates late in *Brassica napus* seed development. *Plant Mol. Biol. 12*, 395–401.
34. Thompson, J. D., Gibson, T. J., Plewniak, F., Jeanmougin, F., and Higgins, D. G. (1997) The CLUSTAL_X windows interface: Flexible strategies for multiple sequence alignment aided by quality analysis tools. *Nucleic Acids Res. 25*, 4876–4882.
35. Chan, W. C., and White, P. D. (2000) in Fmoc solid phase peptide synthesis: A practical approach (Hames, B. D., Ed.) Oxford University Press, Oxford, U.K.
36. Wolkers, W. F., van Kilsdonk, M. G., and Hoekstra, F. A. (1998) Dehydration-induced conformational changes of poly-L-lysine as influenced by drying rate and carbohydrates. *Biochim. Biophys. Acta 1425*, 127–136.
37. Wolkers, W. F., Oliver, A. E., Tablin, F., and Crowe, J. H. (2004) A Fourier-transform infrared spectroscopy study of sugar glasses. *Carbohydr. Res. 339*, 1077–1085.
38. Kawai, H., Kurosaki, K., and Suzuki, T. (2008) Analytical approach for the non-equilibrium state of glassy foods affected by its manufacturing process. *Cryobiol. Cryotechnol. 54*, 71–77 (in Japanese).
39. Tamm, L. K., and Tatulian, S. A. (1997) Infrared spectroscopy of proteins and peptides in lipid bilayers. *Q. Rev. Biophys. 30*, 365–429.
40. Barth, A., and Zscherp, C. (2002) What vibrations tell about proteins. *Q. Rev. Biophys. 35*, 369–430.
41. Haris, P. I., Coke, M., and Chapman, D. (1989) Fourier transform infrared spectroscopic investigation of rhodopsin structure and its comparison with bacteriorhodopsin. *Biochim. Biophys. Acta 995*, 160–167.
42. Heimburg, T., Schuenemann, J., Weber, K., and Geisler, N. (1996) Specific recognition of coiled coils by infrared spectroscopy: Analysis of the three structural domains of type III intermediate filament proteins. *Biochemistry 35*, 1375–1382.
43. Heimburg, T., Schunemann, J., Weber, K., and Geisler, N. (1999) FTIR spectroscopy of multistranded coiled coil proteins. *Biochemistry 38*, 12727–12734.
44. Eom, J., Baker, W. R., Kintanar, A., and Wurtele, E. S. (1996) The embryo-specific EMB-1 protein of *Daucus carota* is flexible and unstructured in solution. *Plant Sci. 115*, 17–24.
45. Lisse, T., Bartels, D., Kalbitzer, H. R., and Jaenicke, R. (1996) The functional benefits of protein disorder. *Biol. Chem. 377*, 555–561.
46. Mouillon, J. M., Gustafsson, P., and Harryson, P. (2006) Structural investigation of disordered stress proteins. Comparison of full-length dehydrins with isolated peptides of their conserved segments. *Plant Physiol. 141*, 638–650.

47. Shih, M. D., Lin, S. C., Hsieh, J. S., Tsou, C. H., Chow, T.,Y., Lin, T. P., and Hsing, Y. I. (2004) Gene cloning and characterization of a soybean (*Glycine max* L.) LEA protein, GmPM16. *Plant Mol. Biol. 56*, 689–703.
48. Dobson, C. M. (2003) Protein folding and misfolding. *Nature 426*, 884–890.
49. Goyal, K., Walton, L. J., and Tunnacliffe, A. (2005) LEA proteins prevent protein aggregation due to water stress. *Biochem. J. 388*, 151–157.
50. Surana, R., Pyne, A., and Suryanarayanan, R. (2004) Effect of aging on the physical properties of amorphous trehalose. *Pharm. Res. 21*, 867–874.
51. Kawai, K., Hagiwara, T., Takai, R., and Suzuki, T. (2005) Comparative investigation by two analytical approaches of enthalpy relaxation for glassy glucose, sucrose, maltose, and trehalose. *Pharm. Res. 22*, 490–495.
52. Crowe, L. M., Reid, D. S., and Crowe, J. H. (1996) Is trehalose special for preserving dry biomaterials? *Biophys. J. 71*, 2087–2093.
53. Matreeve, Y. I., Grinberg, V. Y., Sochava, I. V., and Tolstoguzov, V. B. (1997) Glass transition temperature of proteins. Calculation based on the additive contribution method and experimental data. *Food Hydrocoll. 2*, 125–133.
54. Honjoh, K., Matsumoto, H., Shimizu, H., Ooyama, K., Tanaka, K., Oda, Y., Takata, R., Joh, T., Suga, K., Miyamoto, T., Iio, M., and Hatano, S. (2000) Cryoprotective activities of group 3 late embryogenesis abundant proteins from *Chlorella vulgaris* C-27. *Biosci., Biotechnol. Biochem. 64*, 1656–1663.